ORIGINAL RESEARCH

ED-71 Ameliorates Bone Loss in Type 2 Diabetes Mellitus by Enhancing Osteogenesis Through Upregulation of the Circadian Rhythm Coregulator BMAL1

Ting Liu [ID][1,2], Luxu Wang[1–3], Tuo Shi[4], Hongrui Liu[1,2], Bo Liu[5], Jie Guo [ID][1,2], Minqi Li [ID][1,2,5]

[1]Department of Bone Metabolism, School and Hospital of Stomatology, Cheeloo College of Medicine, Shandong University & Shandong Key Laboratory of Oral Tissue Regeneration & Shandong Engineering Research Center of Dental Materials and Oral Tissue Regeneration & Shandong Provincial Clinical Research Center for Oral Diseases, Jinan, People's Republic of China; [2]Center of Osteoporosis and Bone Mineral Research, Shandong University, Jinan, People's Republic of China; [3]School of Stomatology, Jinzhou Medical University, Jinzhou, People's Republic of China; [4]School of Traditional Chinese Medicine, Beijing University of Chinese Medicine, Beijing, People's Republic of China; [5]School of Clinical Medicine, Jining Medical University, Jining, People's Republic of China

Correspondence: Bo Liu, School of Clinical Medicine, Jining Medical University, Jining, 272067, People's Republic of China, Tel +86-0537-6051782, Email liubo7230@mail.jnmc.edu.cn; Jie Guo, Department of Bone Metabolism, School and Hospital of Stomatology, Cheeloo College of Medicine, Shandong University & Shandong Key Laboratory of Oral Tissue Regeneration & Shandong Engineering Research Center of Dental Materials and Oral Tissue Regeneration & Shandong Provincial Clinical Research Center for Oral Diseases, Jinan, Shandong, 250012, People's Republic of China, Tel +86-0531-88382923, Email kqgj@sdu.edu.cn

Purpose: Bone loss is a common complication of type 2 diabetes mellitus (T2DM). Circadian rhythms play a significant role in T2DM and bone remodeling. Eldecalcitol (ED-71), a novel active vitamin D analog, has shown promise in ameliorating T2DM. We aimed to investigate whether the circadian rhythm coregulator BMAL1 mediates the anti-osteoporotic effect of ED-71 in T2DM and its associated mechanisms.

Methods: A T2DM mouse model was established using high-fat diet (HDF) and streptozotocin (STZ) injection, and blood glucose levels were monitored weekly. HE staining, Masson staining, and Micro-CT were performed to assess the changes in bone mass. IHC staining and IF staining were used to detect osteoblast status and BMAL1 expression and RT-qPCR was applied to detect the change of oxidative stress factors. In vitro, high glucose (HG) stimulation was used to simulate the cell environment in T2DM. RT-qPCR, Western blot, IF, ALP staining and AR staining were used to detect osteogenic differentiation and SIRT1/GSK3β signaling pathway. DCFH-DA staining was used to detect reactive oxygen species (ROS) levels.

Results: ED-71 increased bone mass and promoted osteogenesis in T2DM mice. Moreover, ED-71 inhibited oxidative stress and promoted BMAL1 expression in osteoblasts The addition of STL1267, an agonist of the BMAL1 transcriptional repressor protein REV-ERB, reversed the inhibitory effect of ED-71 on oxidative stress and the promotional effect on osteogenic differentiation. In addition, ED-71 facilitated SIRT1 expression and reduced GSK3β activity. The inhibition of SIRT1 with EX527 partially attenuated ED-71's effects, whereas the GSK3β inhibitor LiCl further enhanced ED-71's positive effects on BMAL1 expression.

Conclusion: ED-71 ameliorates bone loss in T2DM by upregulating the circadian rhythm coregulator BMAL1 and promoting osteogenesis through inhibition of oxidative stress. The SIRT1/GSK3β signaling pathway is involved in the regulation of BMAL1.

Keywords: eldecalcitol, type 2 diabetic mellitus, osteoblast, BMAL1, SIRT1/GSK3β signaling pathway

Introduction

Diabetes mellitus (DM), the third most prevalent chronic metabolic disease, has emerged as a significant worldwide public health concern in the modern world.[1] Type 2 diabetes mellitus (T2DM) constitutes the predominant form, accounting for more than 90% of DM cases, and is associated with complications affecting various organs and tissues, including cardiovascular disease, osteoporosis, and neuropathy.[2,3] The association between T2DM and bone loss has

recently garnered increased attention. The concept of type 2 diabetic osteoporosis (T2DOP) has been proposed, characterized by low bone mass and deterioration of bone microstructure, leading to fragile bones prone to fractures.[4] A recent cohort study revealed prevalence rates of bone loss and osteoporosis in patients with T2DM at 50.6% and 17.7%, respectively.[5] Although patients with T2DM sometimes show an increase in bone mineral density (BMD), the incidence of fractures is significantly increased. A number of studies have noted reduced bone turnover in patients with T2DM, which with decreased osteoblast activity and impaired bone repair.[6] Therefore, targeting to promote osteogenesis is important for the treatment of T2DOP.

The circadian rhythm serves as an endogenous regulator present in the brain and peripheral organs, exhibiting a roughly 24h cycle. The circadian rhythm is generated through the coordinated expression of various clock genes, including brain and muscle Arnt-like protein-1 (BMAL1), circadian locomotor output cycles kaput (CLOCK), crypto-chromes (CRYs), periods (PERs), retinoic acid-associated orphan receptors (RORs), and nuclear receptor subfamily 1 (REV-ERBs). These genes collectively form a transcription-translation feedback loop. BMAL1, serving as a core clock transcriptional factor, forms heterodimers with the CLOCK and targets the classical E-box structure in the promoter region or the non-classical E-box structure in the enhancer region to facilitates the transcription of downstream clock-controlled genes.[7,8] Concurrently, the expression of BMAL1 is modulated by the secondary feedback loop. Within this loop, BMAL1 and CLOCK induce the expression of REV-ERBα and REV-ERBβ. Subsequently, the REV-ERBα/β proteins repress the expression of BMAL1 by competing with the transcriptional activators RORα/γ for the binding to the RORE in the Bmal1 promoter.[9,10] BMAL1 strictly governs multiple physiological and pathological processes of the organism. Mutations in the BMAL1 gene in humans or deletion in mice can cause glucose intolerance and T2DM.[11] BMAL1 overexpression increases insulin secretion and improves glucose tolerance in diet-induced obesity and insulin resistance in mice.[12] Concurrently, in vitro and in vivo experiments have confirmed BMAL1's crucial role in T2DM-related glucose and lipid metabolism disorders and neuropsychiatric damage.[13] Moreover, there is mounting evidence indicating that BMAL1 is essential for the development of hard tissues such as bone, cartilage, and teeth.[14,15] In vivo studies have revealed significant reductions in bone density of the femur and tibia, as well as mandibular deformities in Bmal1 knockout mice. Recent research indicates that the circadian rhythm plays a crucial role in the determination of the fate of mesenchymal stem cells.[16] It has been discovered that bone marrow mesenchymal stem cells isolated from Bmal1 knockout mice have an impaired ability to differentiate into osteoblasts.[17] In vitro, Bmal1 knockdown compromised the osteogenic capacity of bone marrow mesenchymal stem cells, while BMAL1 overexpression promoted osteogenesis.[18] Collectively, these findings underscore the role of BMAL1 in linking glucose metabolism and osteogenesis.

Vitamin D is primarily synthesized endogenously in the skin and obtained from dietary sources. Metabolized by the liver and kidneys into an active form, vitamin D plays a crucial role in the regulation of calcium and phosphorus metabolism and the promotion of bone mineralization.[19] Recently, research interest has grown in the role of vitamin D in regulating circadian rhythm disorders.[20,21] Vitamin D can regulate the decline in oocyte quality and fertility in mice caused by circadian rhythm disruption and prevent skin photo cancer due to UV overexposure.[22,23] It has also been reported that vitamin D can alter the expression of circadian genes in adipose stem cells.[24] Moreover, vitamin D and its derivatives regulate the expression of BMAL1 in the skin cells via Rorα/γ.[25] In turn, CLOCK was able to activate VDR transcription by forming a protein complex with VDR after translocation to the nucleus with the help of BMAL1.[20] All these suggest that vitamin D is closely related to circadian rhythm. Eldecalcitol (ED-71) is a novel active vitamin D analog with hydroxypropyloxy residues at the 2β site, offering a longer half-life in the blood and a reduced risk of calcium-phosphorus imbalance than the original active vitamin D.[26] ED-71 can induce unique "mini-modeling" bone formation, wherein a newly formed bone matrix is directly deposited onto the surface of pre-existing bone without osteoclastic bone resorption.[27] We have previously shown that ED-71 improves bone mass in db/db mice;[4,28,29] however, The mechanism of ED-71 improving bone loss and its beneficial effect in T2DM are still not fully understood.

In this paper, a mouse model of inducible T2DM was established using a high-fat diet (HFD) combined with streptozotocin (STZ) to evaluate the therapeutic effect of exogenous ED-71 supplementation. Given the significant role of circadian rhythm and BMAL1 in T2DM and bone remodeling, as well as the regulation of circadian rhythm by active vitamin D, we focused on the circadian core factor BMAL1 to explore the mechanisms by which ED-71 ameliorates bone loss in T2DM.

Materials and Methods

T2DM Model Establishment and Tissue Preparation

All the animal procedures in this study were performed in accordance with the Guidelines for Care and Use of Laboratory Animals of the National Institutes of Health. All animal experiments were approved by the Institutional Animal Care and Use Committee of the Hospital of Stomatology, Shandong University (No.20230104). 24 8-week-old male C57BL/6J mice, weighing (20 ± 2) g, were purchased from Hangzhou Zhiyuan Laboratory Animal Technology Company and placed in a standard 12h light/dark cycling environment. The light on was defined as Zeitgeber time (ZT) 0 and the light off was defined as ZT12. Mice were randomly divided into a wild-type group (WT group, n = 8) and an experimental group (n = 16). The experimental group was given HFD for 4 weeks, followed by intraperitoneal injection of STZ at a concentration of 100 mg/kg[30] every other day for a total of 2 or 3 times. Fasting blood glucose was measured 2 days after the last injection, and blood glucose higher than 11.1 mmol/L for 3 consecutive days was considered as successful reconstruction of the T2DM model. The WT group continued to be fed routinely, and the animals in the experimental group were randomly divided into two groups: the T2DM group (no treatment) and the T2DM+ED-71 group (ED-71 gavage treatment, 0.25 μg/kg, 3d/week).[31] All mice received drugs at ZT0 each time. Six weeks later, all the mice were anesthetized and underwent cardiac perfusion with 4% paraformaldehyde at ZT4. The femurs were stored in 75% alcohol for micro-computed tomography (Micro-CT) scanning. After being fixed in 4% paraformaldehyde for 1 day, the tibias were decalcified in EDTA-2Na solution at 4°C for 4 weeks, then dehydrated with a series of ethanol gradients, embedded in paraffin, and cut into 5 μm-thick sections for histological analysis. Meanwhile, the left and right forelimbs were used to extract mRNA and protein respectively.

Micro-CT Scan

Samples were dissected aseptically and scanned, and the data were reconstructed using a micro-CT system (Scanco Medical, Wangen-Brüttisellen, Switzerland) to generate three-dimensional images.

Hematoxylin and Eosin (HE) Staining

After dewaxing and hydration, paraffin sections were stained with hematoxylin for 15 min and then stained with eosin for 7 min. Finally, the sections were observed on a light microscope (Olympus BX-53, Tokyo, Japan) and images were acquired.

Masson Staining

After dewaxing and hydration, the sections were soaked in a hematoxylin staining solution for 10 min, soaked in a Ponceau S acid fuchsin solution for 5 min, rinsed in aqueous glacial acetic acid for 2 min, differentiated in aqueous phosphomolybdic acid for 5 min, and then immersed in aniline blue solution for 5 min. Finally, it was observed under the light microscope.

Immunohistochemical (IHC) Staining

Paraffin sections were dewaxed hydrated and placed in 0.3% hydrogen peroxide solution for 30 min. Next, 1% bovine serum albumin-PBS solution (1% BSA-PBS) was added dropwise to block non-specific staining. The corresponding primary antibody, including anti-ALP (ab108337, Abcam) and anti-RUNX2 (ab192256, Abcam), was incubated at 4°C overnight and the corresponding secondary antibody incubated for 1 hour at room temperature. 3,3'-Diaminobenzidine tetrahydrochloride (DAB) was used and the color development was observed under a light microscope and promptly terminated. Sections were restained with 1% methyl green and photographed under the light microscope. Positive expression (optical density, OD) in all sections was analyzed using Image Pro Plus 6.0 software.

Cell Culture and Treatment

Mouse osteoblast cell line MC3T3-E1 provided by Shanghai Cell Centre (Shanghai, China). Cells were cultured in the α-MEM medium with 10% FBS, 100 U/mL penicillin and 100 μg/mL streptomycin. The incubator environment was 37°C

and 5%CO$_2$. Glucose levels were 5.5 mmol/L in the control group (CON group) and 55 mmol/L in the high glucose group (HG group). Cells were pre-synchronised using 100nM dexamethasone stimulation for 2 hours,[32] and the time of synchronisation completion was recorded as circadian time (CT) 0. Cells were treated with 1×10^{-9}M ED-71 (Chugai Pharmaceutical Co., Ltd., Japan),[28] and were respectively collected at CT0, CT6, CT12, CT18, and CT24. Cells were cultured in osteogenic induction conditions (containing 0.1μM dexamethasone, 10mM β-glycerophosphate and 0.05mM ascorbic acid) for 7, 14 or 21 days. For plasmid overexpression experiments, follow the instructions for Lipo8000 Transfection Reagent (C0533, Beyotime). For inhibition experiments, 2mM N-acetylcysteine (NAC) (HY-B0215, MedChemExpress), 5uM STL1267 (HY-148711, MedChemExpress), 10uM EX527 (ab141506, Abcam), and 1mM LiCl (HY-W094474, MedChemExpress) were added to the HG group. Cells were harvested for subsequent experiments.

Reverse Transcriptase-Quantitative PCR (RT-qPCR)

MC3T3-E1 cells were lysed with Trizol reagent (AG21102, Precision Biotechnology). Total RNA was extracted from cell samples using RNAex Pro Reagent (Accurate Biology, Changsha, China). Reverse transcription to cDNA was performed using the Evo M-MLV Reverse Transcription Kit (Accurate Biology, Changsha, China). RT-qPCR was performed in triplicate using a SYBR Green PCR kit (Accurate Biology, Changsha, China) using a real-time PCR system (Bio RAD, Hercules, USA). Relative expression levels of BMAL1, CLOCK, SOD2, Prdx1, GSR, ALP, RUNX 2, OCN, and GAPDH were calculated using the 2$^{-\Delta\Delta Ct}$ method. The levels of the first three factors were normalized to the level of GAPDH. Primer sequences are listed in Table 1.

Western Blot

Total intracellular proteins were extracted by lysing cells using a mixture of RIPA lysate, protease inhibitor, and phosphatase inhibitor (Cwbio, Beijing, China) at a ratio of 99:1:1. Cellular protein concentrations were measured using a BCA kit (P0012S, Beyotime). 30μg proteins were separated in 10% SDS-PAGE and transferred to a PVDF membrane. After washing in 5% BSA-TBST the membranes were co-incubated with primary antibodies: anti-RUNX2 (ab192256, Abcam), anti-OCN (ab93876, Abcam), anti-BMAL1 (14,268-1-AP, Proteintech), anti-Nrf2 (16,396-1-AP, Proteintech), anti-SIRT1 (60,303-1-lg, Proteintech), anti-SOD2 (24,127-1-AP, Proteintech), anti-S9-GSK-3β (AP0039, ABclonal). After overnight incubation with horseradish peroxidase-conjugated goat anti-rabbit IgG (ab6721, Abcam) or goat anti-mouse IgG (SA00001-1, Proteintech) for 1 hour. A gel imaging system (Amersham Imager 600, General Electric Company) was used to generate images. Grey values were analyzed and quantified using Image-Pro Plus 6.0 software (Media Cybernetics) and normalized to GAPDH levels.

Measurement of the Intracellular ROS Level

Intracellular ROS levels were observed by using the fluorescent dye DCFH-DA (S0033, Beyotime). Briefly, treated cells were incubated in α-MEM containing 10μmol/L DCFH-DA for 30 min at 37°C. After washing, images were captured with a fluorescence microscope (DMi8, Leica, Germany). Relative fluorescence intensity was measured using Image J software.

Table 1 Primer Sequences Used in Experiment

Gene	Forward	Reverse
BMAL1	5'-TATCACGCTACGAAGTCGATGGTT-3'	5'-CGCCTTCCAGGACATTGGCTA-3'
CLOCK	5'-CGTTCACTCAGGACAGACAGATAA-3'	5'-GTGTGGCGAAGGTAGGATAGG-3'
SOD2	5'-GCTCTGGCCAAGGGAGAATGTTA-3'	5'-ACCCTTAGGGCTCAGGTTTGTC-3'
Prdx1	5'-AGGTATCTCTTTCAGGGGCCTTT-3'	5'-TATCACTGCCAGGTTTCCAGC-3'
GSR	5'-AGGGCCACATCCTAGTAGACGA-3'	5'-GATTGCAACTGGGGTGAGAAGC-3'
ALP	5'-GCGACCACTTGAGCAAACATC-3'	5'-CGGCTGATTGGCTTCTTCTT-3'
RUNX2	5'-TACGACCATGAGATTGGCAGTGA-3'	5'-TATAGGATCTGGGTGCAGGCTGA-3'
OCN	5'-CAGAACAGACAAGTCCCACACAG-3'	5'-TCAGCAGAGTGAGCAGAAAGAT-3'
GAPDH	5'-GCACCGTCAAGGCTGAGAAC-3'	5'-TGGTGAAGACGCCAGTGGA-3'

Alkaline Phosphatase (ALP) and Alizarin Red (AR) Staining

MC3T3-E1 cells were cultured in the osteogenic induction medium for 7 or 21 days. Cells were fixed in 4% paraformaldehyde for 20 min, then stained with ALP solution (C3206, Beyotime) for 30 min, stained with 1% alizarin red staining solution (G1452, Solarbio) for 15 min. The optical microscope (CKX-41, Olympus Corp., Japan) were used to obtain images.

Immunofluorescence (IF) Staining

After dewaxing and hydration of paraffin sections, the sections were placed in 0.3% hydrogen peroxide solution for 30 min. Cells were fixed with 4% paraformaldehyde, permeabilized with 0.5% Triton X-100. And then 1% or 5% BSA was added dropwise to block non-specific staining. Sections and cells were incubated overnight at 4°C with anti-RUNX2 (ab192256, Abcam), anti-BMAL1 (14,268-1-AP, Proteintech), anti-SIRT1 (60,303-1-lg, Proteintech) and anti-S9-GSK3β (sc-393147, Santa Cruz Biotechnology) primary antibodies. Next day, the fluorescent secondary antibody was incubated for 1 hour at room temperature. Incubate with 4′,6-diamidino-2-phenylindole (DAPI) for 5 min. Images were observed by the fluorescent microscope (DMi8, Leica, Germany).

Statistical Analysis

QQ plots were used to assess data distribution, and when the scatter plot was close to a straight line, it can be considered that the data set was approximately normally distributed. All the quantitative data was expressed as mean ± standard deviation (SD). All experiments were independently repeated at least 3 times. The GraphPad Prism 6.0 software was used to conduct the analysis and the production of pictures for the obtained data. Unpaired two-tailed Student's t-tests were used to compare the means of the two groups, and one-way ANOVA with the Bonferroni post hoc test for multiple comparisons was used to compare the means of the multiple comparisons. $P < 0.05$ was considered statistically significant.

Results

ED-71 Ameliorates Bone Loss in STZ-Induced T2DM Mice in vivo

A T2DM mouse model was established, and bone loss was significantly ameliorated as observed by Micro-CT images of femur after ED-71 treatment. The T2DM group exhibited notably fewer and sparser trabeculae, along with a larger marrow cavity and thinner cortical bone than the WT group. Remarkably, the T2DM+ED-71 group displayed a significant increase in trabecular bone volume, smaller marrow cavities, and restored cortical bone thickness than the T2DM group (Figure 1A). HE staining revealed a significant decrease in the tibial bone volume and trabecular bone number, along with a narrowing of thickness and distribution that became discrete and irregular, in the T2DM group. Moreover, lipid droplets in the marrow cavity significantly increased. In contrast, the T2DM+ED-71 group exhibited increased trabecular bone number and thickness and decreased separation of trabecular bone and lipid droplets (Figure 1B–D). Masson staining demonstrated that bone regeneration significantly decreased in the T2DM group and de novo regeneration increased in the T2DM+ED-71 group (Figure 1C). In addition, continuous weekly monitoring revealed the blood glucose levels gradually decreased in the T2DM+ED-71 group compared with the T2DM group (Figure 1E). Overall, it suggests that ED-71 played a positive role in ameliorating bone loss and controlling blood glucose.

ED-71 Ameliorates HG-Induced Oxidative Stress and Promotes Osteogenesis in vitro and in vivo

Oxidative stress, resulting from an imbalance between reactive oxygen species (ROS) production and antioxidant defense systems, is known to play a significant role in the development and progression of T2DM.[33] Our previous study demonstrated that oxidative stress impairs the differentiation and function of osteoblasts.[34–36] We measured the mRNA expression of key antioxidant genes in bone tissues, including nuclear factor erythroid 2-related factor 2 (Nrf2), superoxide dismutase 2 (SOD2), glutathione reductase (GSR), and peroxiredoxin 1 (Prdx1). Our results showed
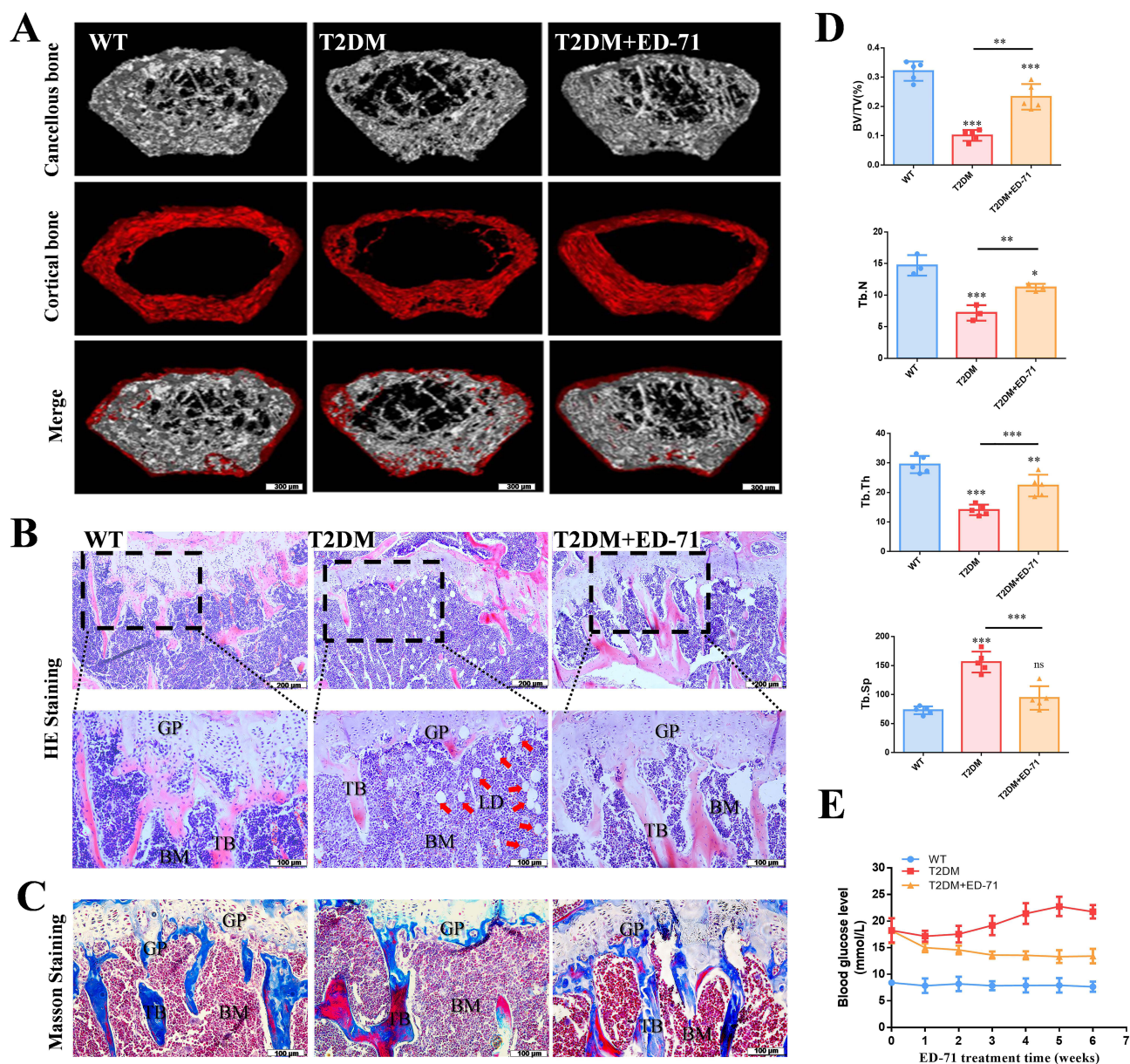
Figure 1 ED-71 ameliorates bone loss in STZ-induced T2DM mice in vivo. (**A**), representative 3D micro-CT images of the femur in different groups, bar = 300μm. (**B**), HE stained images of mouse tibia (n = 5), bar = 200μm or 100μm. Red arrows indicates the position of the LD. (**C**), Masson stained images of mouse tibia (n = 5), bar = 100μm. (**D**), quantitative analysis of bone morphology including bone/tissue volume (BV/TV), trabecular bone number (Tb.N), trabecular bone thickness (Tb.Th) and trabecular separation (Tb.Sp), was performed in different groups using tibial HE staining. (**E**), differences in blood glucose in WT, T2DM, and T2DM + ED-71 groups at 6 weeks of treatment (n = 8). Data are expressed as mean ± SD, * $p < 0.05$, ** $p < 0.01$, *** $p < 0.001$.
Abbreviations: GP, Growth Plate; TB, trabecular bone; BM, bone marrow; LD, lipid droplets.

that the expression of these genes was significantly decreased in the bone tissue of T2DM mice compared with the WT group. Interestingly, treatment with ED-71 significantly increased the levels of Nrf2, SOD2, and Prdx1, indicating a potential antioxidant effect of ED-71 (Figure 2A). Furthermore, the average fluorescence intensity of DCFH-DA staining of MC3T3-E1 cells was significantly increased after exposure to HG stimulation, which indicated elevated ROS levels. Meanwhile, treatment with ED-71 was able to inhibit this increase in ROS levels (Figure 2B and C). Next, we evaluated the effect of ED-71 on the osteoblast differentiation potential in an HG environment. After inducing osteogenic differentiation of MC3T3-E1 cells, we observed a drastic decrease in the mRNA levels of key osteogenic markers, including ALP, runt-related transcription factor 2 (RUNX2), and osteocalcin (OCN), in the HG group. However, treatment with ED-71 led to an increase in the expression levels of these markers, suggesting a promotion of osteoblast
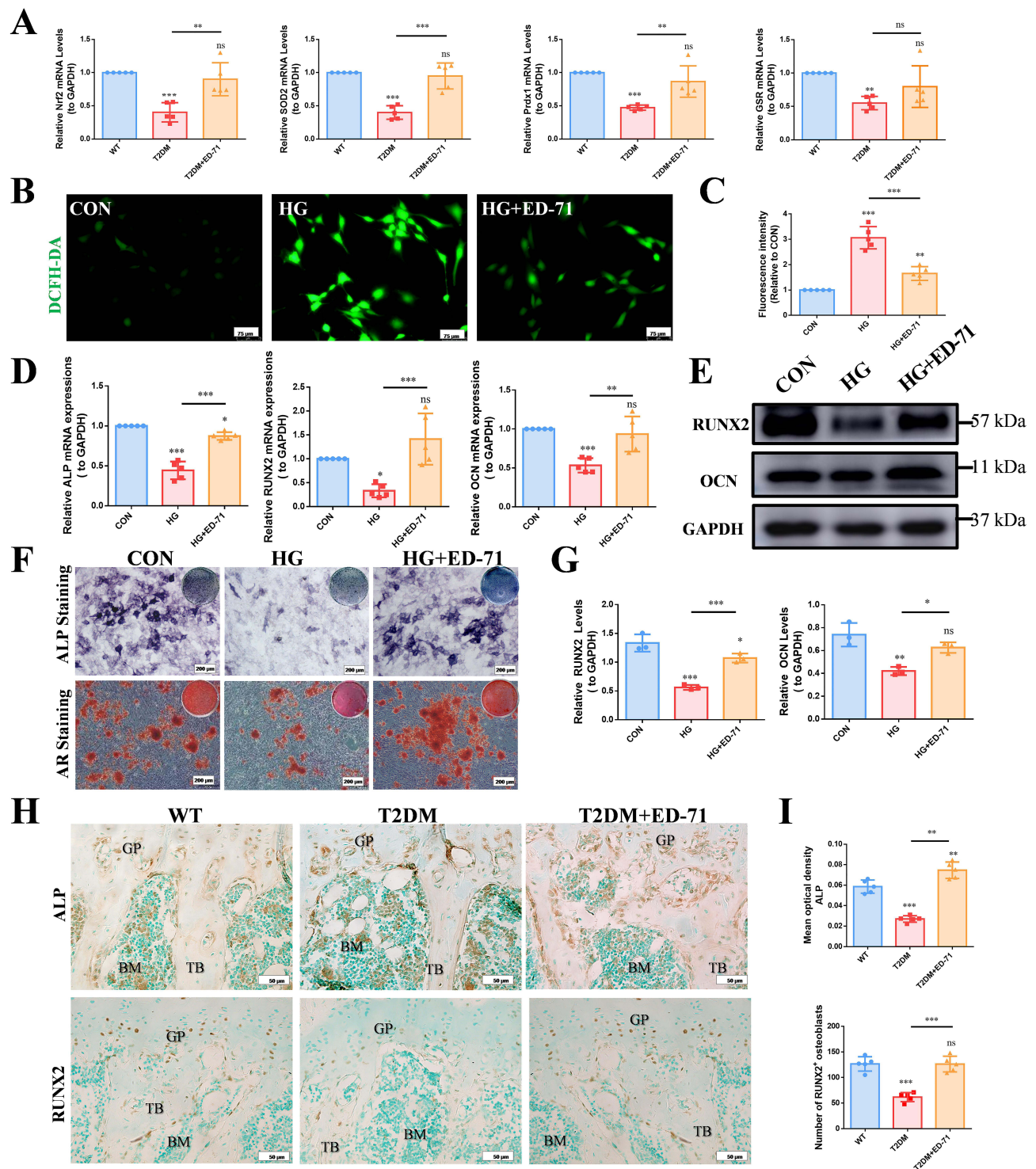
Figure 2 ED-71 ameliorates HG-induced oxidative stress and promotes osteogenic differentiation in vitro and in vivo. (**A**), the mRNA expression of Nrf2, SOD2, and Prdx1 in bone tissues were detected by RT-qPCR in WT, T2DM, and T2DM + ED-71 groups (n = 5). (**B** and **C**), the ROS level in MC3T3-E1 cells was detected by DCFH-DA staining (n = 5), bar = 75μm. (**D**), the mRNA expression of ALP, RUNX2 and OCN in MC3T3-E1 cells after 7 days of culture were detected by RT-qPCR (n = 5). (**E** and **G**) the protein expression of RUNX2 and OCN in MC3T3-E1 cells after 14 days of culture were detected by Western blot. (**F**), ALP staining after 7 days of culture, and AR staining after 21 days of culture of MC3T3-E1 cells in the CON, HG, and HG + ED-71 groups (n = 5), bar = 200μm. (**H** and **I**), IHC staining and statistical analysis of ALP and RUNX2 in tibiae of WT, T2DM, and T2DM + ED-71groups (n = 5), bar = 50μm. Data are expressed as mean ± SD, * $p < 0.05$, ** $p < 0.01$, *** $p < 0.001$.
Abbreviations: GP, Growth Plate; TB, trabecular bone; BM, bone marrow.

differentiation and activity (Figure 2D). These findings were further supported by changes in the protein levels of RUNX2 and OCN (Figure 2E–G). Additionally, ALP and AR staining demonstrated that ED-71 could promote ALP expression and increase the number of calcified nodules (Figure 2F). To validate these results in vivo, we performed IHC detection of ALP and Runx2 expression in the tibia. The results were consistent with the in vitro findings (Figure 2H and I). In conclusion, our results suggest that ED-71 can ameliorate T2DM-induced bone loss by inhibiting oxidative stress and promoting osteogenic differentiation.

ED-71 Promotes BMAL1 Expression to Ameliorate Circadian Rhythm Disturbance of Osteoblasts in vivo and in vitro

The RT-qPCR results of bone tissues showed that the mRNA levels of BMAL1 and CLOCK were significantly reduced in T2DM mice, indicating that the circadian rhythm of bone tissue was disturbed. Notably, BMAL1 levels recovered significantly after ED-71 treatment (Figure 3A). A similar trend in BMAL1 was confirmed by Western blot analysis of bone tissues (Figure 3B–D). Tissue IF double staining showed that the expression of BMAL1 and RUNX2 in osteoblasts was significantly reduced in the T2DM group compared with the WT group, but was partially restored by ED-71 treatment (Figure 3C–E). In vitro Western blot assay and IF staining demonstrated that ED-71 partially restored BMAL1 protein expression in osteoblasts in the HG environment (Figure 3F–I). Continuous 24-hour monitoring results showed that HG could lead to the disturbance of BMAL1 cyclic expression in MC3T3-E1 cells, with sustained low-level shallow amplitude changes, while ED-71 treatment could partially restore the cyclic expression (Figure 3J).

ED-71 Upregulates BMAL1 to Ameliorate Oxidative Stress and Promote Osteoblast Differentiation

A recent study demonstrated that BMAL1 directly controls the transcriptional activity of Nrf2 through the E-box, thereby influencing the expression of its downstream antioxidant genes in Sertoli cells.[37] To clarify the effect of BMAL1 on oxidative stress in osteoblasts, we created a plasmid for BMAL1 overexpression, and the RT-qPCR and Western blot results confirmed successful BMAL1 overexpression in MC3T3-E1 cells (Figure 4A and B). Compared with the vector group, BMAL1 overexpression elevated the mRNA or protein levels of Nrf2, Prdx1 and SOD2 in the HG environment (Figure 4C–E). DCFH-DA staining further indicated that BMAL1 overexpression effectively inhibited the overaccumulation of ROS induced by HG (Figure 4F). REV-ERB is a known transcriptional repressor of BMAL1. STL1267, a REV-ERB agonist, has been proven to effectively inhibit the gene expression of BMAL1.[10] Next, we added STL1267 to the MC3T3-E1 cells during the osteogenic induction. Along with the decrease of mRNA and protein expression of BMAL1, the promotion effect of ED-71 on osteogenic factors such as RUNX2 and osteocalcin was significantly inhibited (Figure 4G–I). In addition, the results of DCFH-DA staining showed that STL1267 partially restored the inhibitory effect of ED-71 on ROS (Figure 4J). Furthermore, ALP staining showed that STL1267 inhibited the promoting effect of ED-71 on osteoblasts, which was in turn rescued by the ROS scavenger NAC (Figure 4K). These findings underscore that BMAL1 may play an important role in mediating the action of ED-71 in inhibiting oxidative stress and promoting osteoblast differentiation.

SIRT1-GSK3β Signaling Pathway is Involved in the Osteoprotective Effect of ED-71 by Upregulating BMAL1 in the HG Environment

Several studies have highlighted the critical role of SIRT1 and GSK3β in circadian rhythm regulation.[38,39] IF staining revealed reduced levels of SIRT1 and S9-GSK3β in MC3T3-E1 cells under an HG environment, while ED-71 significantly enhanced their expression (Figure 5A and B). These findings were consistent with Western blot results (Figure 5C and D). To further clarify whether they are involved in ED-71's effect on BMAL1 in MC3T3-E1 cells, we employed the SIRT1 inhibitor EX-527 and the GSK3β inhibitor LiCl. IF staining showed that EX-527 significantly attenuated the promotion of BMAL1 expression and the inhibition of ROS by ED-71, with this effect further enhanced by LiCl (Figure 5E). Western blot results demonstrated that the reduction in SIRT1 levels caused by EX-527 led to a significant decrease in the protein expression levels of BMAL1, Nrf2, RUNX2, and OCN. Conversely, the addition
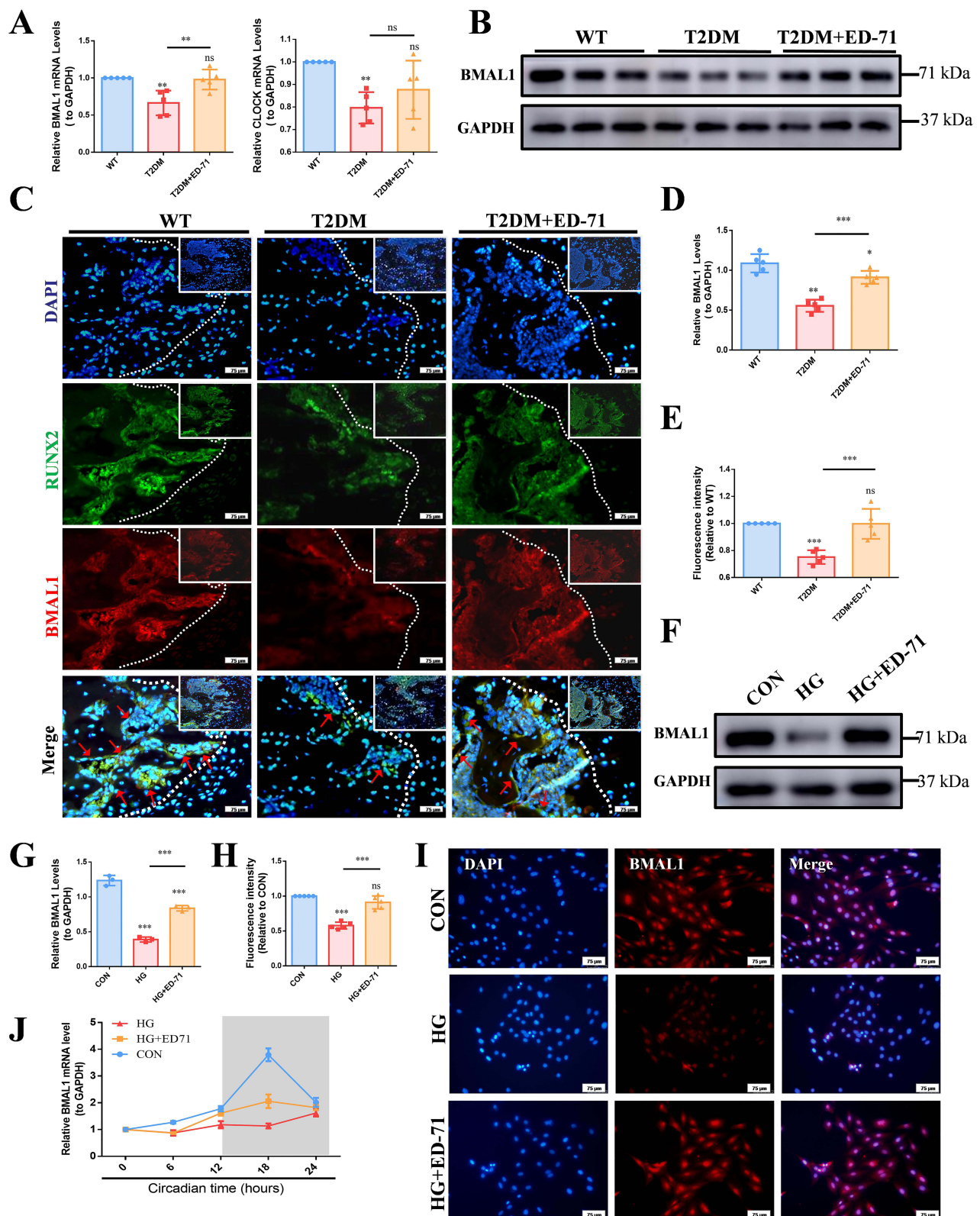
Figure 3 ED-71 promotes BMAL1 expression to ameliorate circadian rhythm disturbances of osteoblasts induced by HG in vivo and in vitro. (**A**), the mRNA expression of BMAL1 and CLOCK in bone tissues were detected by RT-qPCR in WT, T2DM, and T2DM + ED-71groups (n = 5). (**B–D**), Western blot detection and statistical analysis of BMAL1 protein expression in bone tissues (n = 5). (**C** and **E**), representative images of osteogenic gene RUNX2 (green) and rhythmic gene BMAL1 (red) in tibia were observed by IF double staining (n = 5), bar = 75μm. Red arrows indicated the representatives of double positive cells. (**F** and **G**), Western blot detection of BMAL1 protein expression in MC3T3-E1 cells after 48 hours of high glucose stimulation and its statistical analysis (n=3). (**H** and **I**), BMAL1 protein expression in MC3T3-E1 cells detected by IF after 48 hours of high glucose stimulation and its statistical analysis (n = 5), bar = 75μm. (**J**), RT-qPCR to detect changes in BMAL1 mRNA expression within the circadian time for 24 hours after HG stimulation (n = 5). Data are expressed as mean ± SD, * $p < 0.05$, ** $p < 0.01$, *** $p < 0.001$.
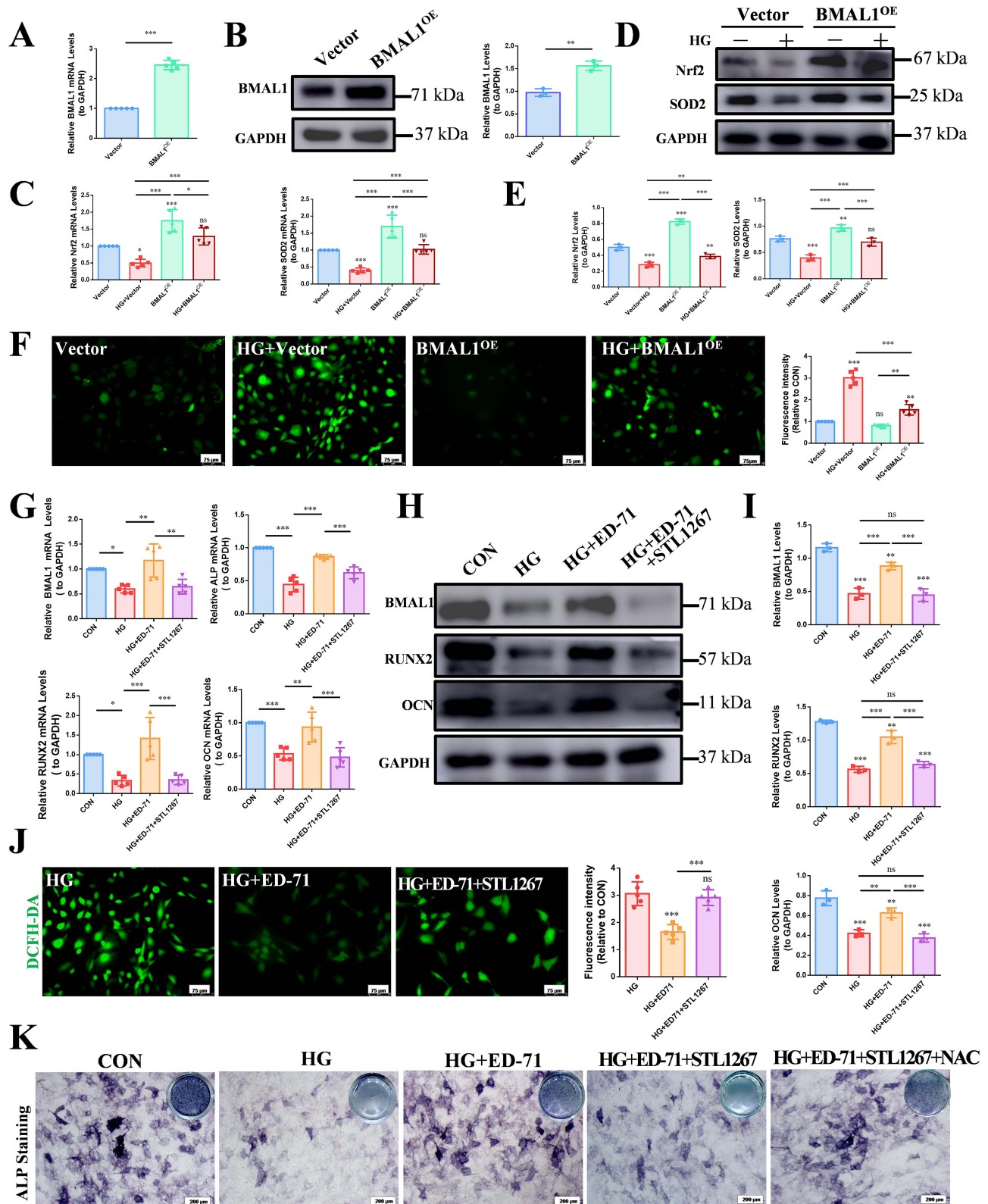
Figure 4 ED-71 upregulates BMAL1 to ameliorate oxidative stress and promote osteoblast differentiation. (**A** and **B**), 48 hours after plasmid transfection, RT-qPCR (n = 5) and Western blot (n = 3) was used to detect the mRNA and protein expression of BMAL1. (**C**), RT-qPCR was used to detect the mRNA of Nrf2 and SOD2 (n = 5). (**D** and **E**), Western blot detection and statistical analysis the protein of Nrf2 and SOD2 (n = 3). (**F**), the ROS level in MC3T3-E1 cells was detected by DCFH-DA staining (n = 5), bar = 75μm. (**G**), the mRNA expression of BMAL1, ALP, RUNX2 and OCN were detected by RT-qPCR after 7 days of culture (n = 5). (**H** and **I**) the protein expression of BMAL1, ALP, RUNX2, and OCN after 14 days of culture was detected by Western blot and statistical analysis (n = 3). (**J**), the ROS level after 48 hours of high glucose stimulation was detected by DCFH-DA staining (n = 5), bar = 75μm. (**K**), ALP staining after 7 days of culture (n = 5), bar = 200μm. Data are expressed as mean ± SD, * *p* < 0.05, ** *p* < 0.01, *** *p* < 0.001.
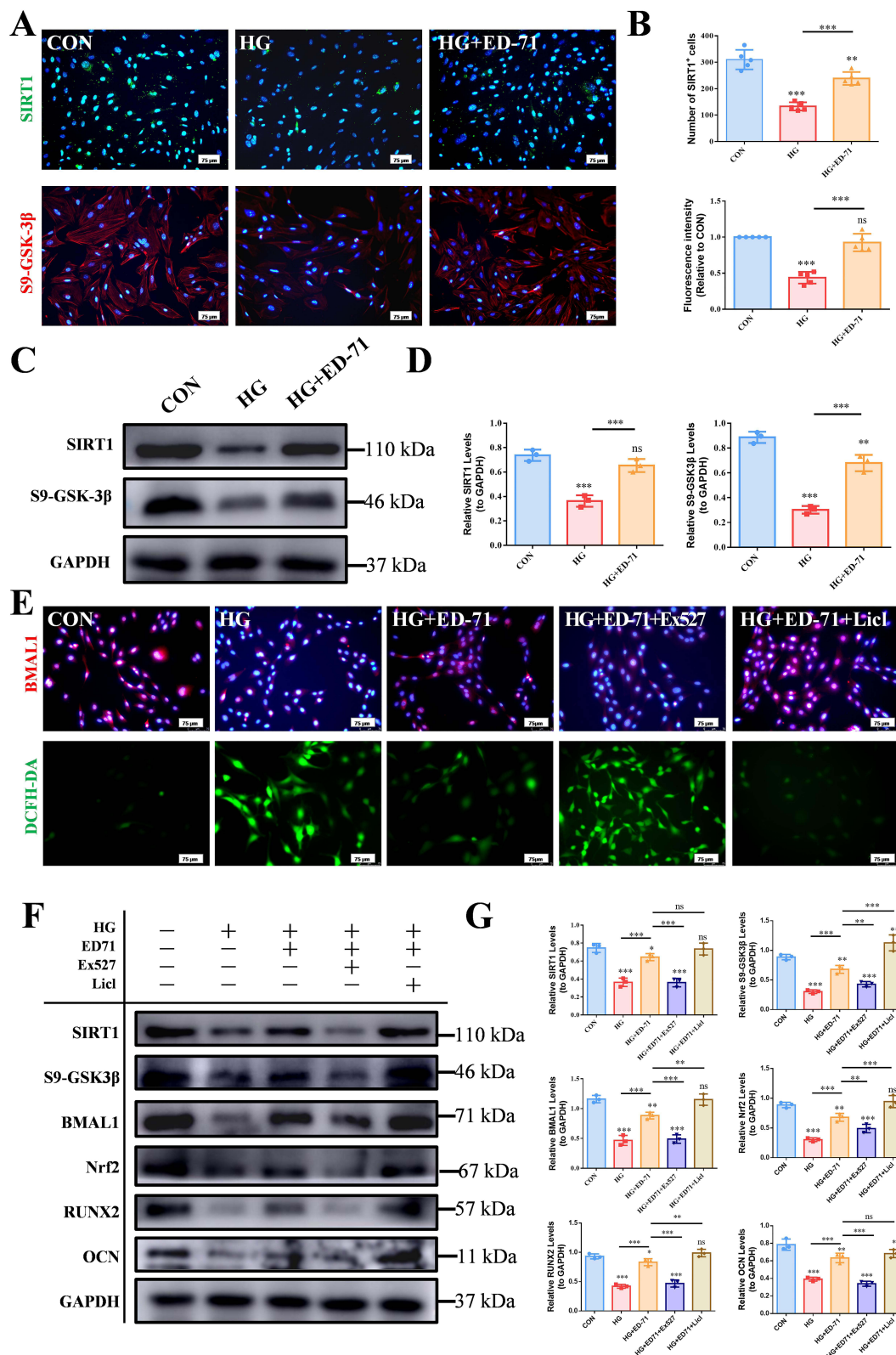
Figure 5 SIRT1-GSK3β signaling pathway is involved in the osteoprotective effect of ED-71 by upregulating BMAL1 in the HG environment. (**A** and **B**), IF staining for SIRT1 and S9-GSK3β observed after 48 hours of HG stimulation and the quantitative analysis (n = 5), bar = 75μm. (**C** and **D**), the protein expression of SIRT1 and S9-GSK3β was detected by Western blot and statistical analysis (n = 3). (**E**), Representative images of BMAL1 and ROS by confocal microscopy (n = 5), bar = 75μm. (**F** and **G**), the protein expression of BMAL1, SIRT1, S9-GSK3β, Nrf2, RUNX2 and OCN was detected by Western blot after 14d culture and statistical analysis (n = 3). Data are expressed as mean ± SD, * $p < 0.05$, ** $p < 0.01$, *** $p < 0.001$.

of LiCl ameliorated the reduction in these factors (Figure 5F and G). Importantly, EX-527 also significantly reduced S9-GSK3β levels, while LiCl had minimal effect on SIRT1 levels (Figure 5F and G). These findings suggest that the SIRT1-GSK3β signaling pathway plays a crucial role in the bone-protective effect of ED-71 by upregulating BMAL1.

Discussion

In this study, we evaluated the effects of ED-71 on bone loss in T2DM and its role in promoting osteogenesis in the HG environment. Our results demonstrate that ED-71 inhibits oxidative stress and promotes osteogenic differentiation by upregulating the circadian rhythm coregulator BMAL1. Additionally, the SIRT1-GSK3β signaling pathway is involved in the upregulation of BMAL1. These findings suggest that rebalancing circadian rhythm is a key mechanism by which ED-71 improves bone loss in T2DM. This not only provided a new direction for further exploring the mechanism of ED-71, but also may offer new therapeutic applications for T2DM and bone loss.

T2DM is a widespread chronic metabolic disease with complex pathophysiological features, including persistent hyperglycemia, insulin resistance, pancreatic β-cell dysfunction, and visceral obesity.[40] Currently, the most commonly used models of T2DM include the spontaneous model represented by leptin receptor-deficient diabetic (db/db) mice and the induced model represented by HFD combined with STZ. The db/db mice, characterized by moderate obesity and severe diabetes mellitus due to leptin receptor mutation.[41] Our previous study found that ED-71 was effective in increasing bone mass and osteogenesis in db/db mice.[4,28,29] While db/db mice exhibit several features of spontaneous T2DM in humans, they do not present pancreatic Amyloid polypeptide deposition which occurs in pancreatic islet tissues of approximately 90% of patients with T2DM, suggesting some pathological distinctions from patients with T2DM.[42] Moreover, T2DM resulting from monogenic mutations is rare in obese individuals, indicating potential limitations in directly extrapolating findings from single-gene mutant animals to human T2DM cases.[43] Additionally, it cannot be ruled out that the specific effects observed in these single-gene mutant animals are associated with obesity or are heavily dependent on leptin signaling.[44] Therefore, to further investigate the effects of ED-71 on T2DM, we established an inducible T2DM mouse model using HFD combined with STZ injection. This model, which does not exhibit obvious obesity characteristics, resembles the acquired growth factors associated with an unhealthy diet and lifestyle prevalent in modern society. Our results showed that the induced mice had abnormally high blood glucose levels and significant bone loss. ED-71 treatment demonstrated a hypoglycemic effect and significantly increased bone volume, trabecular bone number, and new bone regeneration. The induced T2DM mouse model in this study, combined with previously spontaneous db/db mice, suggest that ED-71 may be a potential treatment for T2DM and its complications, including bone loss.

The circadian system comprises a master clock located in the suprachiasmatic nucleus of the hypothalamus and subclocks in peripheral tissues such as the liver, adipose tissue, pancreas, and bone.[45] It is important to understand the broad activity of the circadian system, and how manipulating circadian system could alter metabolism. T2DM is characterized by alterations in the amplitude or timing of various circadian rhythms, including sleep-wake cycles, blood pressure, hormonal rhythms (cortisol and melatonin), and gene expression.[46] As a key regulator of circadian rhythm, BMAL1 plays a crucial role in its generation and maintenance.[47] Bmal1 knockdown mice exhibit abnormalities in blood pressure, glucose homeostasis, lipid metabolism, and adipogenesis, while Bmal1 overexpression increases insulin secretion and glucose tolerance in diet-induced obesity and insulin resistance in mice.[48–50] Abnormal bone metabolism is a common complication of T2DM. Research indicates that bone metabolism follows a typical circadian rhythm, with bone formation predominant during the day and bone resorption dominant at night.[51] Circadian rhythm genes have been identified in osteoblasts and osteoclasts, and disrupted circadian rhythm can lead to an imbalance in bone remodeling.[52] Clinical studies have reported that shift workers, compared with daytime workers, have lower BMD and an increased fracture risk. Basic research has linked abnormal BMAL1 expression to bone-related diseases such as jaw dysplasia, osteoarthritis, and osteoporosis,[15] underscoring the importance of circadian rhythm and BMAL1 in regulating bone remodeling. Our study found reduced BMAL1 expression in the bone tissues of T2DM mice, and further confirmed by IF double staining that it was mainly significantly reduced in osteoblasts. Moreover, in vitro experiments demonstrated that an HG environment can inhibit osteogenic differentiation by downregulating BMAL1 expression in preosteoblasts, which is consistent with previous studies on the relationship between BMAL1 and osteogenesis.

It is well established that oxidative stress impairs the differentiation and function of osteoblasts. Importantly, recent studies have linked BMAL1 to the maintenance of redox homeostasis.[53–55] BMAL1 knockdown affects ROS production in pancreatic β cells enzymatically, thereby impacting their function.[56] BMAL1 reduction leads to redox imbalance and mitochondrial

dysfunction in HepG2 cells.[54] Nrf2, a transcription factor, mediates the production of antioxidant genes to balance cellular oxidation states, including SOD2, Prdx1, and GSR. Nrf2 levels and activity are known to be under circadian control,[57] with the BMAL1-CLOCK heterodimer directly regulating Nrf2 transcriptional activity by binding to the E-box in the promoter region.[37,58] Our study showed that HG led to decreased BMAL1 expression along with elevated ROS levels in MC3T3-E1 cells. Additionally, antioxidant factors Nrf2 and its downstream enzymes SOD2 and Prdx1 were reduced, and these changes were effectively reversed by BMAL1 overexpression. Our study highlights that BMAL1 has an important role in inhibiting oxidative stress and that it may be a potential target for the treatment of bone loss in T2DM.

A growing body of research indicates a strong association between vitamin D and circadian rhythm. Low vitamin D levels have been linked to sleep disorders.[59] Vitamin D regulates melatonin production, the main hormone involved in sleep regulation, by promoting the conversion of tryptophan into melatonin precursors.[60] Studies show that a vitamin D-deficient diet can lead to circadian rhythm disorders in the liver.[61] Active vitamin D alters the expression of circadian genes such as Bmal1 and Per2 in adipose-derived stem cells.[24] Furthermore, vitamin D and its derivatives regulate BMAL1 expression in skin cells through the Rorα/γ pathway.[25] ED-71, a novel active vitamin D analog, shows promising application prospects compared with traditional vitamin D. While previous research has demonstrated that ED-71 can regulate oxidative stress and osteogenic differentiation, the mechanisms involved are unclear. The effects of ED-71 on circadian rhythms have not been studied. This study fills this gap by showing that ED-71 promotes the expression of BMAL1, a core regulator of circadian rhythm, in bone tissue of T2DM mice and MC3T3-E1 cells under HG conditions.

SIRT1, a member of the NAD+-dependent deacetylase family, is an important target for many drugs that improve circadian rhythm, such as resveratrol[62] and melatonin.[63] Moreover, the inhibition of GSK3β promotes BMAL1 expression by degrading REV-ERBα, a negative regulator of BMAL1, through the ubiquitin-dependent proteasome pathway.[64] In our study, we identified SIRT1 and GSK3β as key regulators of BMAL1 modulation by ED-71. Inhibition of SIRT1 counteracted the upregulation of BMAL1 induced by ED-71, while inhibition of GSK3β intensified this effect, suggesting a complex interplay between these signaling pathways in the context of BMAL1 regulation. Several other studies have also demonstrated a link between SIRT1 and GSK3β. For example, EX-527 greatly reduced S9-GSK3β levels and enhanced GSK3β activity in podocytes under HG conditions.[65] The renal protective effect of nicotinamide adenine dinucleotide was shown to be mediated by regulating GSK-3β in a SIRT1-dependent manner.[66] SIRT1 affects mycobacterial growth by promoting GSK3β phosphorylation; pretreatment with GSK3β phosphorylation inhibitors reduces this effect.[67] Our results showed that EX-527 significantly decreased S9-GSK3β levels, suggesting that SIRT1 acts as an upstream signal to modulate GSK3β activity, consistent with previous findings. Although our findings reveal that ED-71 can partially rebalance circadian rhythm by promoting BMAL1 expression through the SIRT1/GSK3β pathway, the precise mechanism by which this signaling regulates the circadian protein BMAL1 remains to be elucidated, and the role of ED-71 in other circadian factors warrants further investigation.

Overall, we initially clarified that BMAL1 is a key factor in ED-71's role in inhibiting oxidative stress to promote bone formation. However, it must be acknowledged that because circadian rhythm can broadly affect multiple metabolic pathways, inappropriate manipulation of circadian rhythm may lead to unforeseen side effects. Therefore, in future studies, we need to comprehensively assess the potential risks associated with circadian rhythm manipulation to ensure the safety of ED-71 in clinical applications of T2DM.

Conclusion

Our study highlights the significant association between circadian rhythm disorders and bone loss in T2DM. We provide compelling evidence that ED-71 attenuates bone loss in T2DM by inhibiting oxidative stress and promoting bone formation through the restoration of BMAL1 expression, mediated by the SIRT1/GSK3β signaling pathway (Figure 6). These findings suggest that rebalancing the circadian rhythm may be one of the key roles of ED-71, which not only provides a new direction for further exploration of the mechanisms of ED-71, but may also provide new therapeutic ideas for T2DM and bone loss.
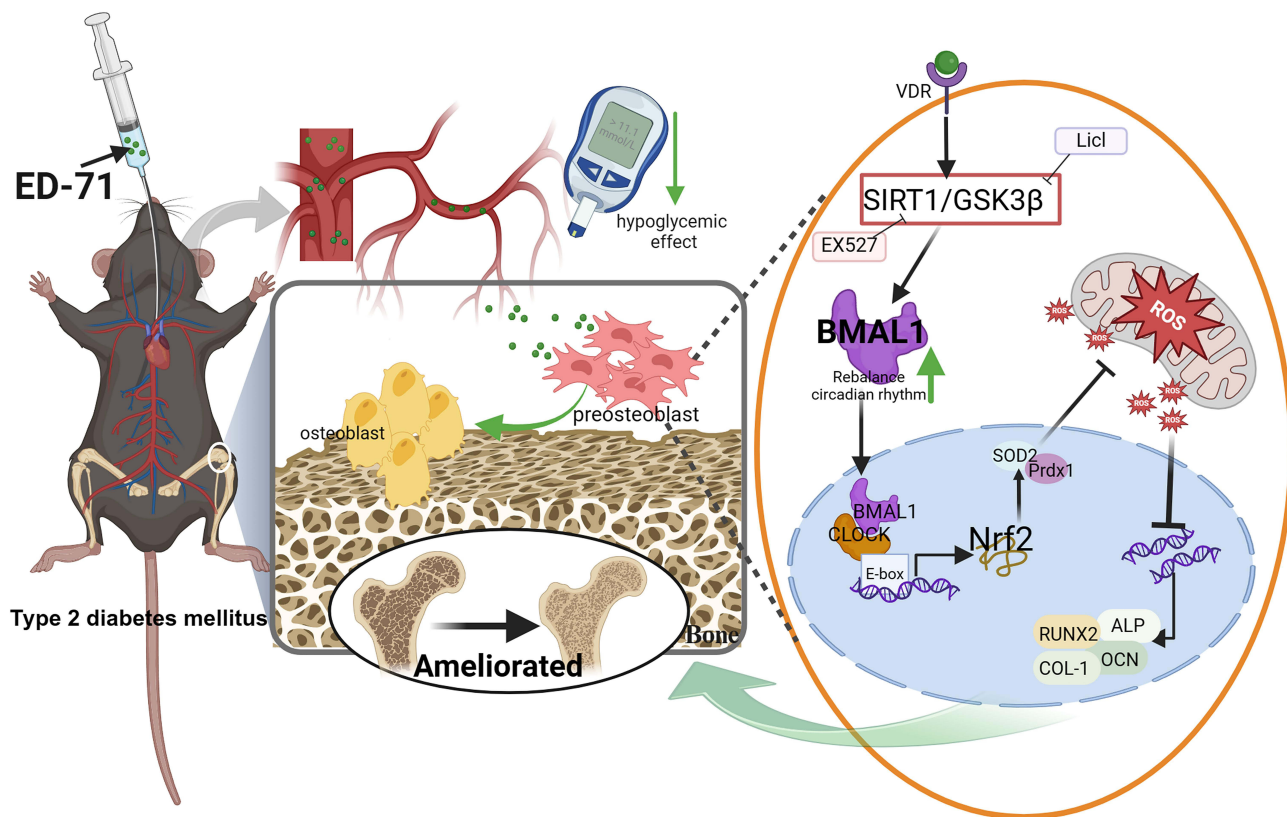
Figure 6 Model diagram of ED-71 ameliorating bone loss in T2DM through upregulation BMAL1. ED-71 ameliorates bone loss in T2DM by inhibiting oxidative stress and promoting bone formation through the restoration of the circadian rhythm coregulator BMAL1 expression, mediated by the SIRT1/GSK3β signaling pathway.

Ethical Approval

All the animal procedures in this study were performed in accordance with the Guidelines for Care and Use of Laboratory Animals of the National Institutes of Health. All animal experiments were approved by the Institutional Animal Care and Use Committee of the Hospital of Stomatology, Shandong University (No.20230104).

Author Contributions

All authors made a significant contribution to the work reported, whether that is in the conception, study design, execution, acquisition of data, analysis and interpretation, or in all these areas; took part in drafting, revising or critically reviewing the article; gave final approval of the version to be published; have agreed on the journal to which the article has been submitted; and agree to be accountable for all aspects of the work.

Funding

Disclosure

The authors declare that they have no conflicts of interest with the contents of this article.

References

1. Li L, Xie J, Zhang Z, et al. Recent advances in medicinal and edible homologous plant polysaccharides: preparation, structure and prevention and treatment of diabetes. *Int J Biol Macromol*. 2023;258(Pt 2):128873. doi:10.1016/j.ijbiomac.2023.128873

2. Zheng Y, Ley SH, Hu FB. Global aetiology and epidemiology of type 2 diabetes mellitus and its complications. *Nat Reviews Endocr*. 2018;14 (2):88–98. doi:10.1038/nrendo.2017.151

3. Liu X, Chen F, Liu L, Zhang Q. Prevalence of osteoporosis in patients with diabetes mellitus: a systematic review and meta-analysis of observational studies. *BMC Endocr Disord*. 2023;23(1):1. doi:10.1186/s12902-022-01260-8

4. Shi T, Liu T, Kou Y, et al. The synergistic effect of zuogui pill and eldecalcitol on improving bone mass and osteogenesis in type 2 diabetic osteoporosis. *Medicina*. 2023;59(8). doi:10.3390/medicina59081414

5. Zhang W, Li Y, Li S, et al. Associations of metabolic dysfunction-associated fatty liver disease and hepatic fibrosis with bone mineral density and risk of osteopenia/osteoporosis in T2DM patients. *Front Endocrinol*. 2023;14:1278505. doi:10.3389/fendo.2023.1278505

6. Tonks KT, White CP, Center JR, et al. Bone turnover is suppressed in insulin resistance, independent of adiposity. *J Clin Endocrinol Metab*. 2017;102(4):1112–1121. doi:10.1210/jc.2016-3282

7. Fan R, Peng X, Xie L, et al. Importance of Bmal1 in Alzheimer's disease and associated aging-related diseases: mechanisms and interventions. *Aging Cell*. 2022;21(10):e13704. doi:10.1111/acel.13704

8. Kiyohara YB, Nishii K, Ukai-Tadenuma M, et al. Detection of a circadian enhancer in the mDbp promoter using prokaryotic transposon vector-based strategy. *Nucleic Acids Res*. 2008;36(4):e23. doi:10.1093/nar/gkn018

9. Yu F, Wang Z, Zhang T, et al. Deficiency of intestinal Bmal1 prevents obesity induced by high-fat feeding. *Nat Commun*. 2021;12(1):5323. doi:10.1038/s41467-021-25674-5

10. Murray MH, Valfort AC, Koelblen T, et al. Structural basis of synthetic agonist activation of the nuclear receptor REV-ERB. *Nat Commun*. 2022;13 (1):7131. doi:10.1038/s41467-022-34892-4

11. Rakshit K, Hsu TW, Matveyenko AV. Bmal1 is required for beta cell compensatory expansion, survival and metabolic adaptation to diet-induced obesity in mice. *Diabetologia*. 2016;59(4):734–743. doi:10.1007/s00125-015-3859-2

12. Rakshit K, Matveyenko AV. Induction of core circadian clock transcription factor bmal1 enhances β-cell function and protects against obesity-induced glucose intolerance. *Diabetes*. 2021;70(1):143–154. doi:10.2337/db20-0192

13. Gao X, Wei Y, Sun H, et al. Role of bmal1 in type 2 diabetes mellitus-related glycolipid metabolic disorder and neuropsychiatric injury: involved in the regulation of synaptic plasticity and circadian rhythms. *Mol Neurobiol*. 2023;60(8):4595–4617. doi:10.1007/s12035-023-03360-5

14. Yu S, Tang Q, Chen G, et al. Circadian rhythm modulates endochondral bone formation via MTR1/AMPKβ1/BMAL1 signaling axis. *Cell Death Differ*. 2022;29(4):874–887. doi:10.1038/s41418-021-00919-4

15. Chen G, Tang Q, Yu S, et al. The biological function of BMAL1 in skeleton development and disorders. *Life Sci*. 2020;253:117636. doi:10.1016/j.lfs.2020.117636

16. Gao W, Li R, Ye M, et al. The circadian clock has roles in mesenchymal stem cell fate decision. *Stem Cell Res Ther*. 2022;13(1):200. doi:10.1186/s13287-022-02878-0

17. Samsa WE, Vasanji A, Midura RJ, Kondratov RV. Deficiency of circadian clock protein BMAL1 in mice results in a low bone mass phenotype. *Bone*. 2016;84:194–203. doi:10.1016/j.bone.2016.01.006

18. Jinteng L, Peitao X, Wenhui Y, et al. BMAL1-TTK-H2Bub1 loop deficiency contributes to impaired BM-MSC-mediated bone formation in senile osteoporosis. *Mole Therap - Nucleic Acid*. 2023;31:568–585. doi:10.1016/j.omtn.2023.02.014

19. Janoušek J, Pilařová V, Macáková K, et al. Vitamin D: sources, physiological role, biokinetics, deficiency, therapeutic use, toxicity, and overview of analytical methods for detection of vitamin D and its metabolites. *Crit Rev Clin Lab Sci*. 2022;59(8):517–554. doi:10.1080/10408363.2022.2070595

20. Kawai M, Kinoshita S, Yamazaki M, et al. Intestinal clock system regulates skeletal homeostasis. *JCI Insight*. 2019;4. 10.1172/jci.insight.121798.

21. Hassan N, McCarville K, Morinaga K, et al. Titanium biomaterials with complex surfaces induced aberrant peripheral circadian rhythms in bone marrow mesenchymal stromal cells. *PLoS One*. 2017;12(8):e0183359. doi:10.1371/journal.pone.0183359

22. Li A, Li F, Song W, et al. Gut microbiota-bile acid-vitamin D axis plays an important role in determining oocyte quality and embryonic development. *Clin Trans Med*. 2023;13(10):e1236. doi:10.1002/ctm2.1236

23. Lamnis L, Christofi C, Stark A, et al. Differential regulation of circadian clock genes by UV-B radiation and 1,25-dihydroxyvitamin D: a pilot study during different stages of skin photocarcinogenesis. *Nutrients*. 2024;16(2):254. doi:10.3390/nu16020254

24. Gutierrez-Monreal MA, Cuevas-Diaz Duran R, Moreno-Cuevas JE, Scott SP. A role for 1α,25-dihydroxyvitamin d3 in the expression of circadian genes. *J Biol Rhythms*. 2014;29(5):384–388. doi:10.1177/0748730414549239

25. Slominski AT, Kim TK, Takeda Y, et al. RORα and ROR γ are expressed in human skin and serve as receptors for endogenously produced noncalcemic 20-hydroxy- and 20,23-dihydroxyvitamin D. *FASEB J*. 2014;28(7):2775–2789. doi:10.1096/fj.13-242040

26. Saito H, Kakihata H, Nishida Y, et al. The safety and effectiveness profile of eldecalcitol in a prospective, post-marketing observational study in Japanese patients with osteoporosis: interim report. *J Bone Miner Metab*. 2017;35(4):456–463. doi:10.1007/s00774-016-0779-2

27. de Freitas PH, Hasegawa T, Takeda S, et al. Eldecalcitol, a second-generation vitamin D analog, drives bone minimodeling and reduces osteoclastic number in trabecular bone of ovariectomized rats. *Bone*. 2011;49(3):335–342. doi:10.1016/j.bone.2011.05.022

28. Lu Y, Liu S, Yang P, et al. Exendin-4 and eldecalcitol synergistically promote osteogenic differentiation of bone marrow mesenchymal stem cells through M2 macrophages polarization via PI3K/AKT pathway. *Stem Cell Res Ther*. 2022;13(1):113. doi:10.1186/s13287-022-02800-8

29. Gao R, Zhang W, Jiang Y, et al. Eldecalcitol effectively prevents alveolar bone loss by partially improving Th17/Treg cell balance in diabetes-associated periodontitis. *Front Bioeng Biotechnol*. 2023;11:1070117. doi:10.3389/fbioe.2023.1070117

30. Tu P, Huang B, Li M, et al. Exendin-4 may improve type 2 diabetes by modulating the epigenetic modifications of pancreatic histone H3 in STZ-induced diabetic C57BL/6 J mice. *J Physiol Biochem*. 2022;78(1):51–59. doi:10.1007/s13105-021-00835-8

31. Hirota Y, Nakagawa K, Isomoto K, et al. Eldecalcitol is more effective in promoting osteogenesis than alfacalcidol in Cyp27b1-knockout mice. *PLoS One*. 2018;13(10):e0199856. doi:10.1371/journal.pone.0199856

32. Takarada T, Xu C, Ochi H, et al. Bone resorption is regulated by circadian clock in osteoblasts. *J Bone Miner Res*. 2017;32(4):872–881. doi:10.1002/jbmr.3053

33. Chen J, Wang Q, Li R, et al. The role of sirtuins in the regulatin of oxidative stress during the progress and therapy of type 2 diabetes mellitus. *Life Sci*. 2023;333:122187. doi:10.1016/j.lfs.2023.122187

34. Liu S, Du J, Li D, et al. Oxidative stress induced pyroptosis leads to osteogenic dysfunction of MG63 cells. *J Mol Histol*. 2020;51(3):221–232. doi:10.1007/s10735-020-09874-9

35. Du J, Feng W, Sun J, et al. Ovariectomy upregulated the expression of peroxiredoxin 1 &5 in osteoblasts of mice. *Sci Rep*. 2016;6(1):35995. doi:10.1038/srep35995

36. Kou Y, Rong X, Tang R, et al. Eldecalcitol prevented OVX-induced osteoporosis through inhibiting BMSCs senescence by regulating the SIRT1-Nrf2 signal. *Front Pharmacol*. 2023;14:1067085. doi:10.3389/fphar.2023.1067085

37. Zhang Z, Cheng J, Yang L, et al. The role of ferroptosis mediated by bmal1/Nrf2 in nicotine -induce injury of BTB integrity. *Free Radic Biol Med*. 2023;200:26–35. doi:10.1016/j.freeradbiomed.2023.02.024

38. Liu L, Cao Q, Gao W, et al. Melatonin ameliorates cerebral ischemia-reperfusion injury in diabetic mice by enhancing autophagy via the SIRT1-BMAL1 pathway. *FASEB J*. 2021;35(12):e22040. doi:10.1096/fj.202002718RR

39. Tan H, Zhu Y, Zheng X, et al. PIWIL1 suppresses circadian rhythms through GSK3β-induced phosphorylation and degradation of CLOCK and BMAL1 in cancer cells. *J Cell & Mol Med*. 2019;23(7):4689–4698. doi:10.1111/jcmm.14377

40. Xourafa G, Korbmacher M, Roden M. Inter-organ crosstalk during development and progression of type 2 diabetes mellitus. *Nat Rev Endocrinol*. 2024;20(1):27–49. doi:10.1038/s41574-023-00898-1

41. Kleinert M, Clemmensen C, Hofmann SM, et al. Animal models of obesity and diabetes mellitus. *Nat Rev Endocrinol*. 2018;14(3):140–162. doi:10.1038/nrendo.2017.161

42. Hsu CC, Templin AT, Prosswimmer T, et al. Human islet amyloid polypeptide-induced β-cell cytotoxicity is linked to formation of α-sheet structure. *Protein Sci*. 2023;e4854. 10.1002/pro.4854.

43. O'Rahilly S. Human genetics illuminates the paths to metabolic disease. *Nature*. 2009;462(7271):307–314. doi:10.1038/nature08532

44. Lutz TA. Mammalian models of diabetes mellitus, with a focus on type 2 diabetes mellitus. *Nature Reviews Endocrinology*. 2023;19(6):350–360. doi:10.1038/s41574-023-00818-3

45. Mohawk JA, Green CB, Takahashi JS. Central and peripheral circadian clocks in mammals. *Annu Rev Neurosci*. 2012;35(1):445–462. doi:10.1146/annurev-neuro-060909-153128

46. Brown MR, Sen SK, Mazzone A, et al. Time-restricted feeding prevents deleterious metabolic effects of circadian disruption through epigenetic control of β cell function. *Sci Adv*. 2021;7(51):eabg6856. doi:10.1126/sciadv.abg6856

47. Zheng Y, Pan L, Wang F, et al. Neural function of Bmal1: an overview. *Cell Biosci*. 2023;13(1):1. doi:10.1186/s13578-022-00947-8

48. Petrenko V, Stolovich-Rain M, Vandereycken B, et al. The core clock transcription factor BMAL1 drives circadian β-cell proliferation during compensatory regeneration of the endocrine pancreas. *Genes Dev*. 2020;34(23–24):1650–1665. doi:10.1101/gad.343137.120

49. Sadacca LA, Lamia KA, deLemos AS, et al. An intrinsic circadian clock of the pancreas is required for normal insulin release and glucose homeostasis in mice. *Diabetologia*. 2011;54(1):120–124. doi:10.1007/s00125-010-1920-8

50. Nakata M, Kumari P, Kita R, et al. Circadian Clock Component BMAL1 in the Paraventricular Nucleus Regulates Glucose Metabolism. *Nutrients*. 2021;14(1):13. doi:10.3390/nu13124487

51. Tian Y, Ming J. The role of circadian rhythm in osteoporosis; a review. *Front Cell Develop Biol*. 2022;10:960456. doi:10.3389/fcell.2022.960456

52. Swanson C. Sleep Disruption and bone health. *Curr Osteoporosis Rep*. 2022;20(3):202–212. doi:10.1007/s11914-022-00733-y

53. Nagasaka Y, Nakamura Y, Tran NQV, et al. Deficiency of BMAL1 promotes ROS generation and enhances IgE-dependent degranulation in mast cells. *Biochem Biophys Res Commun*. 2024;690:149295. doi:10.1016/j.bbrc.2023.149295

54. Zhang W, Ho CT, Lu M. Piperine improves lipid dysregulation by modulating circadian genes bmal1 and clock in HepG2 cells. *Int J Mol Sci*. 2022. doi:10.3390/ijms23105611

55. Rabinovich-Nikitin I, Rasouli M, Reitz CJ, et al. Mitochondrial autophagy and cell survival is regulated by the circadian Clock gene in cardiac myocytes during ischemic stress. *Autophagy*. 2021;17(11):3794–3812. doi:10.1080/15548627.2021.1938913

56. de Jesus DS, Bargi-Souza P, Cruzat V, et al. BMAL1 modulates ROS generation and insulin secretion in pancreatic β-cells: an effect possibly mediated via NOX2. *Mol Cell Endocrinol*. 2022;555:111725. doi:10.1016/j.mce.2022.111725

57. Early JO, Menon D, Wyse CA, et al. Circadian clock protein BMAL1 regulates IL-1β in macrophages via NRF2. *Proc Natl Acad Sci USA*. 2018;115(36):E8460–e8468. doi:10.1073/pnas.1800431115

58. Pekovic-Vaughan V, Gibbs J, Yoshitane H, et al. The circadian clock regulates rhythmic activation of the NRF2/glutathione-mediated antioxidant defense pathway to modulate pulmonary fibrosis. *Genes Dev*. 2014;28(6):548–560. doi:10.1101/gad.237081.113

59. de Menezes-Júnior LAA, Sabião TDS, de Moura SS, et al. Influence of sunlight on the association between 25-hydroxyvitamin D levels and sleep quality in Brazilian adults: a population-based study. *Nutrition*. 2023;110:112008. doi:10.1016/j.nut.2023.112008

60. Huiberts LM, Smolders K. Effects of vitamin D on mood and sleep in the healthy population: interpretations from the serotonergic pathway. *Sleep Med Rev*. 2021;55:101379. doi:10.1016/j.smrv.2020.101379

61. Li R, Wang G, Liu R, et al. Quercetin improved hepatic circadian rhythm dysfunction in middle-aged mice fed with vitamin D-deficient diet. *J Physiol Biochem*. 2023;80(1):137–147. doi:10.1007/s13105-023-00990-0

62. Jiang J, Gu Y, Ding S, et al. Resveratrol reversed ambient particulate matter exposure-perturbed oscillations of hepatic glucose metabolism by regulating SIRT1 in mice. *Environ Sci Pollut Res Int*. 2023;30(11):31821–31834. doi:10.1007/s11356-022-24434-2

63. Yin XL, Li JC, Xue R, et al. Melatonin pretreatment prevents propofol-induced sleep disturbance by modulating circadian rhythm in rats. *Exp Neurol*. 2022;354:114086. doi:10.1016/j.expneurol.2022.114086

64. Yin L, Wang J, Klein PS, Lazar MA. Nuclear receptor rev-erbalpha is a critical lithium-sensitive component of the circadian clock. *Science*. 2006;311(5763):1002–1005. doi:10.1126/science.1121613

65. Su PP, Liu DW, Zhou SJ, et al. Down-regulation of risa improves podocyte injury by enhancing autophagy in diabetic nephropathy. *Military Med Res*. 2022;9(1):23. doi:10.1186/s40779-022-00385-0

66. He S, Gao Q, Wu X, et al. NAD + ameliorates endotoxin-induced acute kidney injury in a sirtuin1–dependent manner via GSK-3β/Nrf2 signalling pathway. *J Cell & Mol Med*. 2022;26(7):1979–1993. doi:10.1111/jcmm.17222

67. Yang H, Chen J, Chen Y, et al. Sirtuin inhibits M. tuberculosis -induced apoptosis in macrophage through glycogen synthase kinase-3β. *Arch Biochem Biophys*. 2020;694:108612. doi:10.1016/j.abb.2020.108612